Original Article

MODFLOW/MT3DMS based modeling leachate pollution transfer in solid waste disposal of Bahar plain deep aquifer

Abdollah Taheri Tizro[1*] Behzad Sarhadi[2] Mohamad Mohamadi[3]

1. Associate Professor of Hydrogeology, Department of Water Science Engineering, Faculty of Agriculture, Bu-Ali Sina University, Hamedan, Iran
2. MSc of Water Resources Engineering, Department of Water Science Engineering, Faculty of Agriculture, Bu-Ali Sina University, Hamedan, Iran
3. MSc of Water Resources Engineering, Department of Water Science Engineering, Faculty of Agriculture, Bu-Ali Sina University, Hamedan, Iran

***Correspondence to**: Abdollah Taheri Tizro
ttizro@yahoo.com

(Received: 11 Dec. 2017; Revised: 17 Feb. 2018; Accepted: 28 Apr. 2018)

Abstract

***Background and purpose*:** This paper presents a case study in simulation of process governing leachate occurrence and subsequent transport, and investigates its migration away from the landfill to control environmental adverse effects on a deep aquifer.

***Materials and Methods*:** The landfill examined in this study was an area of 240 ha and received 500 ton/day of solid waste generated from Hamedan and its surrounding including Bahar, and Jurghan. Based on the finite difference technique, leachate transport and penetration into the Hamedan plain aquifer was simulated exerting MODFLOW and MT3DMS codes in GMS Software.

***Results*:** It was concluded that landfill geological structure had the greatest influence on the transfer of urban solid waste leachate in traditional disposal sites. A low permeable conglomerate layer prohibited leachate migration to the main semi-confined aquifer. The results also indicated that urban solid waste leachate was only excited to migrate toward recharging waterways of aquifer by surface flows flooding as well as severe rainfalls.

***Conclusion*:** Geological structure of the landfill area had the greatest influence on the development of leachate pollution of municipal solid waste in traditional disposal sites. The spread of pollution to the deep aquifer near the waste disposal site was practically inhibited by an impermeable conglomerate layer in the municipal waste disposal.

***Keywords*:** Ground Water Pollution; Landfill; Municipal Solid Waste; MODFLOW; MT3DMS
Citation*: Taheri Tizro A, Sarhadi B, Mohamad Mohamadi M. MODFLOW/MT3DMS based modeling leachate pollution transfer in solid waste disposal of Bahar plain deep aquifer 2018; 6 (2): 11-30.

1. Introduction

Economic and social considerations including rapid urbanization, increasing population levels, the rise in the community living standards, and booming economy have greatly made acceleration in the municipal solid waste generation rate (17). Municipal solid waste collection and management is an issue of critical importance facing city planner's worldwide (23). The problem is an increasing burdensome challenge in developing countries, where lack of adequate resources and environmental technologies along with urbanization and poor planning contribute to the inefficient and uncontrolled solid waste management (16).

In both industrial and developing countries, landfills have historically been considered as a final way to store waste at minimum cost. Therefore, landfilling is the most common waste management solution to storage and process of waste generated by increasing urbanization of humans and industries (10). When landfilling, leachate is formed, mainly due to the rainwater infiltration through the refuse tips. In other words, leachate is the result of water contact with the solid waste.

Leachate generation and management have currently become as one of the major environmental problems associated with the operation of sanitary landfills, because the subsequent migration of liquid wastes away from landfill boundaries can cause notable contamination issues by releasing to the adjacent environments, such as surface waters, ground, and soil, therefore liquid wastes are considered major pollution hazards to public health and safety unless precautionary measures are applied (22). The aim of the present research was to investigate leachate occurrence and subsequent transport, and its migration away from the landfill, and its adverse effects on a deep aquifer of Bahar and adjoining Plain by simulation process based on the finite difference technique. The landfill examined in this study was an area of 240 ha and received 500 ton/day of solid waste.

2. Materials and Methods

2.1. Study area

Municipal solid waste of Hamedan plain, once the site of hydrogeological units of Hamadan, is located 20 km north east of Hamedan. Since the beginning of its operation, it has been planned for development over an area of 240 ha. From the viewpoint of geographical location, the study area lies within the longitude range of 34° 57' 21" to 34° 58' 17" and latitude range of 48° 35' 50" to 48° 37' 94". The study area is bounded by Hamedan-Tehran road from the north, Hamedan plain from the North East, Nehran village from the south, and finally Ghatargoni Mountains from the West. Currently, it receives about 500 ton/day and 5 ton/day of household and hospital produced wastes, respectively in Hamadan, Bahar, and Jurghan. These solid wastes are accumulated in an ordinary and infectious specified disposal sites in the natural earth morphology irrespective of sanitary landfilling considerations including creating proper infrastructure and basic preliminary and final impermeable coverage (Figure 1) (21).

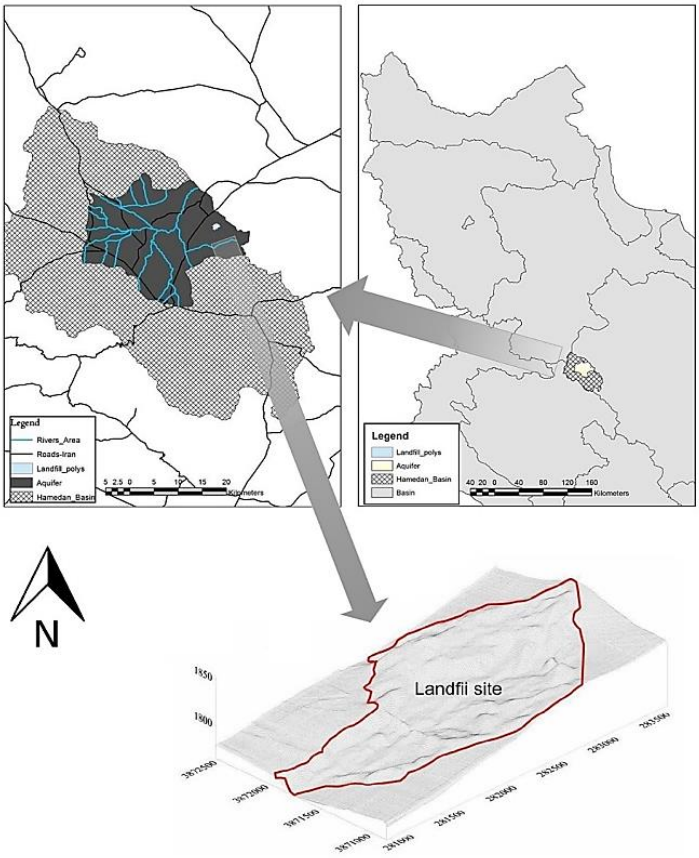

Figure 1. Geographical location of municipal solid waste landfill on drainage basins map (grade 2), Hamedan, Iran (21)

Hydrological characteristics of the study area

A reconnaissance survey of the study area revealed that relatively horizontal conglomerates cover Qom formation with moderate degree of consolidation (14). Based on previous studies (21), a borehole with a depth of 10 m has been excavated in the west of the mentioned landfill in order to subsurface explorations. The log investigation revealed that thickness of the alluvial deposits on top of the conglomerate is about 4.4 m (Figures 2 and 3).

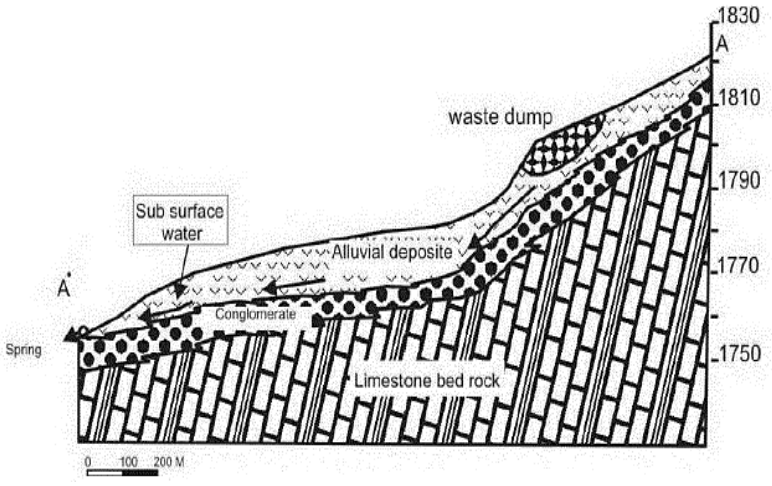

Figure 2. Cross-section of the landfill (21)

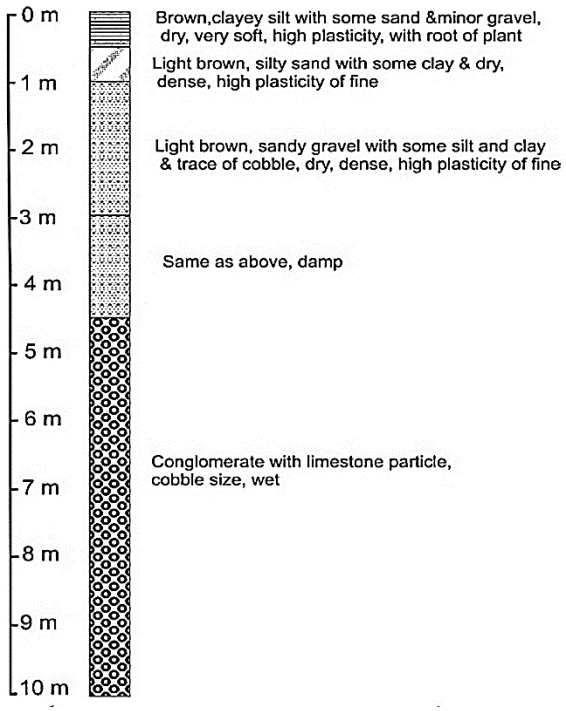

Figure 3. Excavation log in west of the landfill (21)

The study area is composed of a shallow aquifer in quaternary alluvial deposits, which is segregated from a deep aquifer via a low permeable conglomerate unit. In fact, the deep aquifer has been formed in the limestone bedrock and its thickness is expanding toward West (Hamedan plain). The advent of spring and subsurface water depletion are only observed in positions with conglomerate layer which appears at earth surface (1, 21).

2.2. *Methodology*

Performance of MODFLOW and MT3DMS codes

Three-dimensional groundwater transfer in porous media can be described utilizing the following partial differential equation in the MODFLOW family codes:

$$\frac{\partial}{\partial x}\left(K_{xx}\frac{\partial h}{\partial x}\right)+\frac{\partial}{\partial y}\left(K_{yy}\frac{\partial h}{\partial y}\right)+\frac{\partial}{\partial z}\left(K_{zz}\frac{\partial h}{\partial z}\right)-W = S_s\frac{\partial h}{\partial t} \quad (1)$$

Where x, y, z (m) are the principle coordinate axes of the system, k_{xx} , k_{yy} , k_{zz} (m/s) are the principle hydraulic conductivities, W (1/s) is the volumetric heat flux per unit volume and represents sources or sinks of water, S_s (1/s) is the specific storage, h (m) is the hydraulic head, and t (s) represents the time. Equation (1) characterizes the flow along three orthogonal axes in heterogeneous and anisotropic aquifers. For MODFLOW code, a three-dimensional finite difference grid system was formed by simple blocks. Figure 4 demonstrates a spatial discretization of the aquifer system, which is formed by blocks. Hence, an (i, j, k) coordinate system that is a compatible computer array was applied. Cell (i, j, k) and its six adjacent cells and indices in an aquifer are depicted in Figure 4. Based on Darcy's law, the flow rate from cell (i, j-1, k) into cell (i, j, k) in the row direction is defined as follows (6):

$$q_{i.j-\frac{1}{2}.k} = KR_{i.j-\frac{1}{2}.k}\Delta C_i \Delta v_k \frac{(h_{i.j-1.k} - h_{i.j.k})}{\Delta r_{j-\frac{1}{2}}} \quad (2)$$

Where $q_{i,j-\frac{1}{2},k}$ (m^3/s) is the flow rate through the face between cells (i, j, k) and (i, j-1, k), $KR_{i.j-\frac{1}{2}.k}$ (m/s) is the hydraulic conductivity in the entire region between nodes of (i, j, k) and (i, j-1, k), $\Delta r_{j-\frac{1}{2}}$ (m) is the distance between nods of (i, j, k) and (i, j-1, k). Similarly, Equation (2) can be written for the flow rate into or out of the cell via the remaining five faces specified in Figure 4. This equation is simplified by combination of network dimensions and hydraulic conductivity coefficients as follows (6):

$$q_{i.j-\frac{1}{2}.k} = CR_{i.j-\frac{1}{2}.k}(h_{i.j-1.k} - h_{i.j.k}) \quad (3)$$

Where $CR_{i.j-\frac{1}{2}.k}$ (m^2/s) is the conductance in row i and layer k between nodes of (i, j, k) and (i, j-1, k).

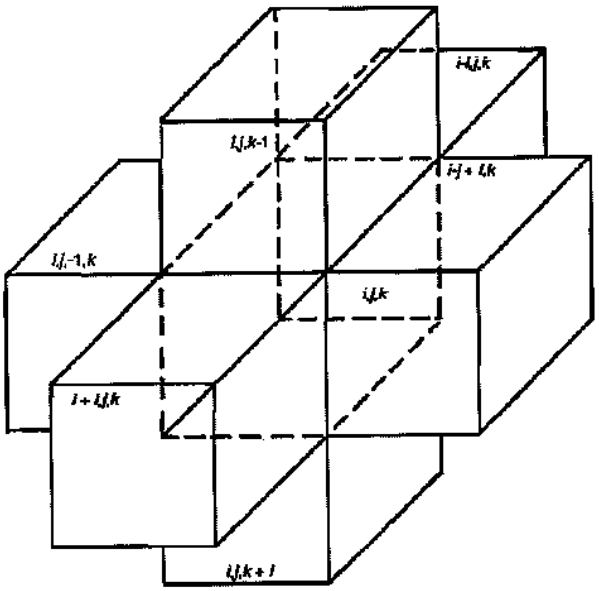

Figure 4. Cell (i, j, k) and its six adjacent cells and indices in an aquifer (6)

In MODFLOW mathematical code, flow from the outside of the aquifer is expressed using Equation (4) (6):

$$a_{i.j.k.n} = p_{i.j.k.n}h_{i.j.k} + q_{i.j.k.n} \quad (4)$$

Where $a_{i.j.k.n}$ (m^3/s) is the flow rate from *nth* external source through cell (i, j, k), and $p_{i.j.k.n}h_{i.j.k}$ and $q_{i.j.k.n}$ (m^3/s) are constants. Therefore, according to the whole continuity equation, the external flow rate of cell (i, j, k) can be defined as follows (6):

$$q_{i.j-\frac{1}{2}.k} + q_{i.j+\frac{1}{2}.k} + q_{i-\frac{1}{2}.j.k} + q_{i+\frac{1}{2}.j.k} + q_{i.j.k-\frac{1}{2}} + q_{i.j.k+\frac{1}{2}} = \sum Q \quad (5)$$

Where $\sum Q$ (m^3/s) represents the flow rate between cell (i, j, k) and its six neighboring nodes. Equation (6) yields the continuity equation containing the flow rate of cell (i, j, k) and the external flow rate (6):

$$\sum Q + QS_{i.j.k} = S_{s_{i.j.k}} \frac{\Delta h_{i.j.k}}{\Delta t} \Delta r_j \Delta c_i \Delta v_k \quad (6)$$

Where $QS_{i.j.k}$ (m^3/s) is the general flow from the cell (i, j, k), $S_{s_{i.j.k}}$ (1/m) is the specific storage of the cell (i, j, k), $\frac{\Delta h_{i.j.k}}{\Delta t}$ (m/s) is the finite difference approximation of head change regarding time, and $\Delta r_j \Delta c_i \Delta v_k$ (m^3) is the volume of cell (i, j, k).

The water level hydrograph in nodes i, j and k are demonstrated in Figure 5, which is characterized by two specified time values on the horizontal axis and their corresponded head values on the vertical axis. When analyzing Equation (7), t_m (s) is defined as the water level value in the nodes i, j and k with $h^m_{i.j.k}$ corresponding head value and time interval extending backward as much as Δt_m changes the corresponding head value from $h^m_{i.j.k}$ to $h^{m-1}_{i.j.k}$. Therefore, the Equation (7) is introduced in the backward difference approximation technique (6):

$$\left(\frac{\Delta h_{i.j.k}}{\Delta t}\right)_m = \frac{(h^m_{i.j.k} - h^{m-1}_{i.j.k})}{(t_m - t_{m-1})} \quad (7)$$

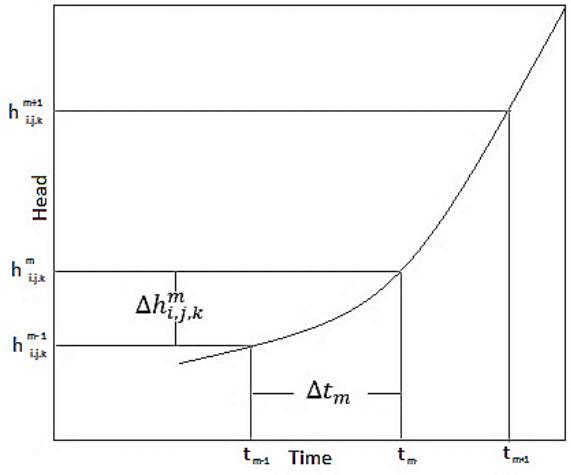

Figure 5. Finite difference approximation in backward technique (6)

Backward finite difference relationship is considered as a fundamental correlation for simulation of groundwater partial derivatives via substituting the Equation (7) in Equation (6) (6). According to Equation (7), due to the end of the time step and seven unknown head levels at time t_m that are to be predicted, there is no possibility of independent solution. In an additional effort, computational modeling converts the set of parameters of Equation (7) into "n" number equations in "n" unknown parameters by identifiable solution of these equations for all network active cells. Cells activation in the initial modeling employing conceptual model, which is a favor of current research, requires accuracy in data entry and adequate selection of modeling approaches. Therefore, the conceptual model must converge in its initial implementation. Then, the leachate transfer from surface is simulated using MT3DMS

mathematical code and backward finite difference technique based on the equation governing the pollution transfer (Equation (8)).

$$\frac{\partial(\theta C^k)}{\partial t} = \frac{\partial}{\partial x_i}\left(\theta D_{ij}\frac{\partial C^k}{\partial x_j}\right) - \frac{\partial}{\partial x_i}(\theta v_i C^k) + q_s C_s^k + \sum R_n \quad (8)$$

Where θ (dimensionless) is the porosity, C^k (dimensionless) is the concentration of the soluble of pollutant k, D_{ij} (dimensionless) is the tensor of the hydraulic dispersion coefficient, t (s) is the time, x_i and x_j (m) are the principle distances on the Cartesian system, v_i (m/s) is the velocity of the water flow in porous media or the Darcy velocity, q_s (m^3/s) is the volumetric flow rate per unit volume of the aquifer, C_s^k (dimensionless) is the concentration of the pollutant k in the flow in borehole and spring, and $\sum R_n$ is the chemical reaction unit. With respect to the Equation (8), simulation of the transfer model is only calibrated on a groundwater flow quantitative model. In accordance with the minimal statistical bias of parameters affecting the flow rate and considering the most accurate conceptual convergent model, the transfer model calibration is more probable (31).

Model conceptualization of geological structure

Over the past few years, nine boreholes have been excavated with a total height of 827 m in Hamedan plain. Table 1 gives information about excavated logs utilized in the final solid production (18). Based on the maps characterizing the surface geological layers of the study area (11, 14), the information of each excavated borehole was justified regarding the significance of upper layers in direct contact with the waste disposal sites.

Table 1. The geographical position of the final solid borehole (18)

Name	x	Y	DEM
Hesam Abad	264145	3873559	1744
Dehpiaz	271600	3864000	1722
Lalehjn	268884	3879010	1752
Shorin	276000	3854800	1795
University 1	277294	3858380	1784
University 2	277102	3859087	1774
BH	279808	3872657	1737
A1	282531	3871688	1803
A2	281095	3873023	1767

Considering a total number of 98 boreholes (primary and hypothetical), a new three-dimensional solid structure was then produced by imaging system maintenance and minimizing cellular thickness (Figures 6 and 7).

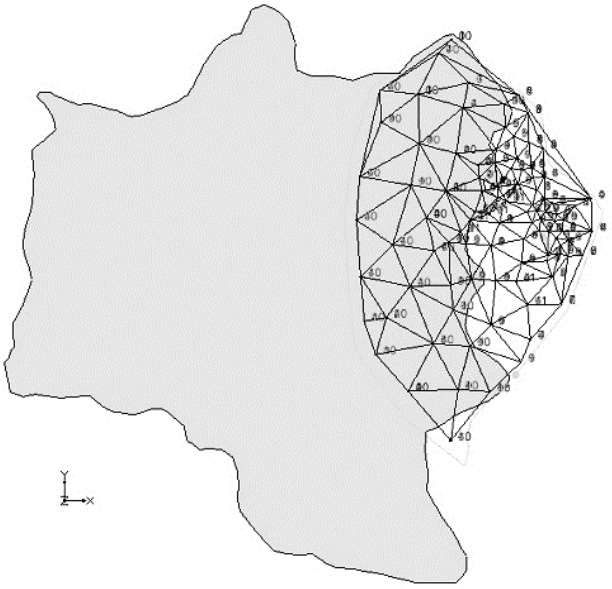

Figure 6. Geological structure modification of the study area by increasing the hypothetical boreholes on the primary solid

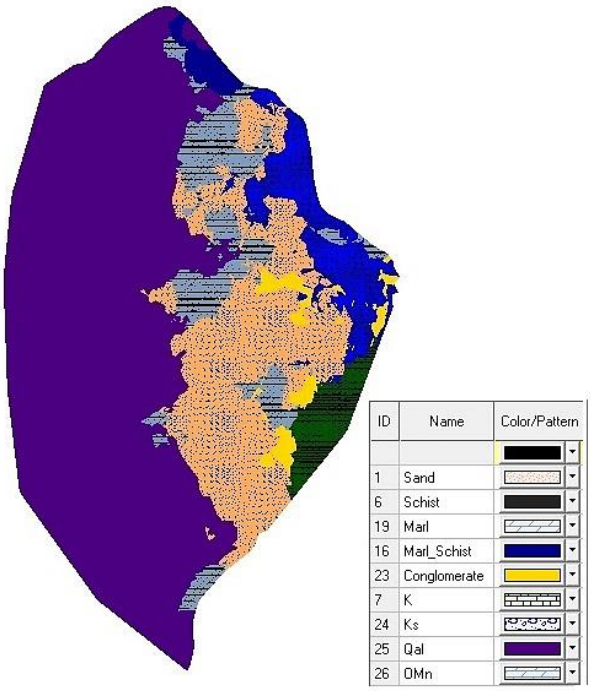

Figure 7. Solid structure and its composition in boreholes (11, 14)

The Grid definition is only credible in the areas adjacent to the Hamedan waste disposal sites toward the areas contacting the aquifer. The existence of layers with a maximum thickness of 3 m and an average depth of 13 m in geological structure necessitates the determination of at least five horizontal layers within the landfill for Grid mathematical model (5).

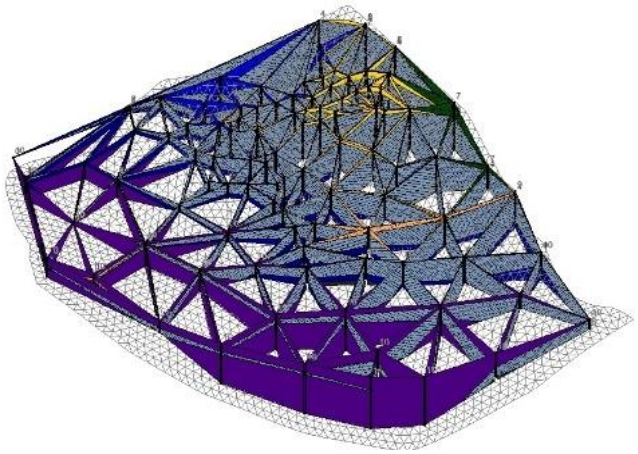

Figure 8. Structure modification of cross-section considering each material defined in the study area based on preliminary Solid

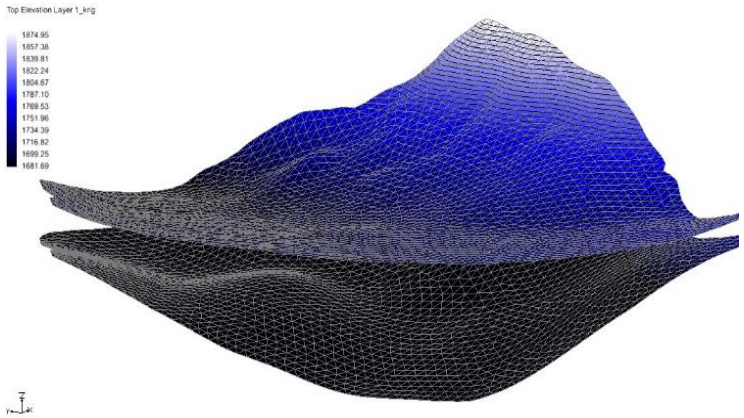

Figure 9. Earth surface and bedrock meshing in the study area

Horizontal hydraulic conductivity parameter was previously estimated at each point using the contour lines with transfer susceptibility after interpolation by Krijing approach in Grid and considering aquifer saturation thickness using pumping experiments and reconnaissance surveys of Geological and Regional water departments. The storage coefficient values were also calculated (Equation (8)) in the form of krijing interpolation of counter lines in Grid Parameters, which were then directly transferred to Grid using Solid structure (Figure 10).

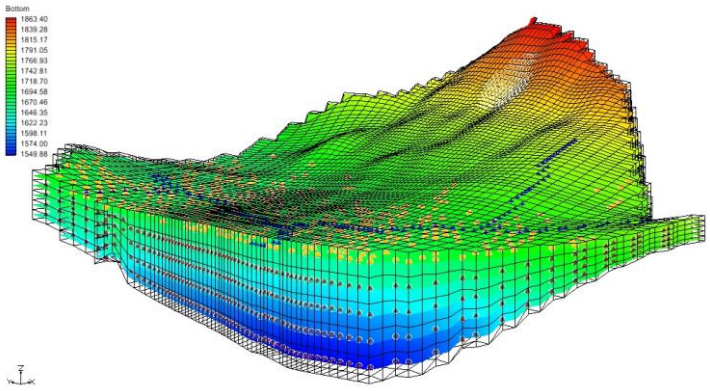

Figure 10. Geological structure of transmission of Solid to Grid

The average vertical hydraulic conductivity of each ingredient was obtained in accordance with its composition (12, 19). The parameter was then estimated in alluvial materials for each ingredient based on Harlman equation and effective particles size (D10). Vertical hydraulic conductivity was found to be equivalent to the 0.1 of the horizontal hydraulic conductivity in the mass center of the non-alluvial materials (24,2).

3. Results

Conceptual model

Taking into account the penetration of 20% of the overall surface of the aquifer, the volume of recharge water is annually equivalent to 31.43×10^6 m^3**.** Considering the evaporation rate, the water volume which returns to the ground was estimated to be 21765.29307 m^3/day (30%) in the agricultural applications and 21461.93102 m^3/day (45%) in the urban purposes, respectively. For transient modeling of leachate transfer toward the deep bed aquifer, 20% penetrated rainfall water was added to the total of returned water to the ground. In the study area, drainage network consists of seasonal and permanent rivers with the importance priority belonging to the Abshineh River. Considering the specific hydrometric information of daily and peak flow rates within the study range, the primary guesstimate of the bed thickness, and transfer susceptibility of bed material, this element was added to the conceptual model with the nature of river (31). 456 exploitation and 12 observational boreholes were also defined in the conceptual model. The boundary conditions were then implemented in accordance with counter and flow lines.

Model calibration

Calibration necessity was determined regarding the sensitivity of MT3DMS qualitative modeling and its dependency on the simulation accuracy in quantitative part of the flow (Eq. (8)). Inverse modeling process was also performed by introducing uncertain parameters applying PEST automated method (7). In this way, the model was characterized using the key number -200 and 36 pilot points with the same point's distribution across the range of minimum and maximum initial guess of horizontal hydraulic conductivity parameter. In addition, the initial estimation about vertical hydraulic conductivities were characterized within the range of minimum and maximum of more and less than one second of initial value by defining a unique key number for each of the solid structural materials (Tables 2 and 3).

Table 2. Result of Vertical hydraulic conductivity estimation and calculation of eight defined materials in final Solid structure (12, 19)

Soil	Key	Material		Diameter	Harlman	Horizontal K (Centroid)
				D10 (cm)	M/Day	Saturated Hydraulic Conductivity, K (M/Day)
Sand - Qt2	-400	Young alluvial terraces	Medium sand 9×10-7 to 5×10-4 Fine sand 2×10-7 to 2×10-4 Silt, loess 1×10-9 to 2×10-5	0.002	0.22149919	1.091621
Schist	1E-10	Schist	Schist	-	-	1E-10
Marl	-401	Clay or limestone	Karst and reef limestone 1×10-6 to 2×10-2 Clay 1×10-11 to 4.7×10-9	0.003	0.49837317	1.4337955
Marl_Schist	-402	Marl Schist	Schist Conglomerate	-	-	0.71689775
Conglomerate	1E-10	Conglomerate	Conglomerate	-	-	1E-10
K	-403	Inseparable cretaceous: Lime+ shale+ sandstone	Karst and reef limestone 1×10-6 to 2×10-2 Sandstone 3×10-10 to 6×10-6 Shale 1×10-13 to 2×10-9	-	-	0.853859
Ks	-404	Sandstone+ dolomite sandstone+ conglomerate	Limestone, dolomite 1×10-9 to 6×10-6	-	-	4.492631
Qal	-405	Alluvium: sand+ sandstone pebble+ Conglomerate	Coarse sand 9×10-7 to 6×10-3 Medium sand 9×10-7 to 5×10-4	0.006	1.99349268	6.9294545
OMn	-401	Clay or limestone	Karst and reef limestone 1×10-6 to 2×10-2 Clay 1×10-11 to 4.7×10-9	0.003	0.49837317	1.4337955

Table 3. Optimized hydraulic conductivity and specific discharge values (7,19, 24)

Soil	VK_Key	Optimized Value	SY_Key	Optimized Value
Sand - Qt2	-400	0.0029941	-600	0.14967
Schist	1E-10	1E-10	-601	0.26
Marl	-401	0.33646	-602	0.344049
Marl Schist	-402	0.0887242	-603	0.1595
Conglomerate	1E-10	1E-10	-604	0.05
K	-403	0.057459	-605	0.12667
Ks	-404	0.55217	-606	0.08175
Qal	-405	1.141	-607	0.159
OMn	-401	0.33646	-602	0.344049

To verify the calibration step, demonstration of the relative error (RMS) and the graph of the correlation between the observed and computed values are given in Figures 11 and 12. Eq. (9) corresponds to the association between the regression line in the correlation graph, where the coefficient of determination was estimated to be $R^2 = 0.9978$.

$$y = 0.9913x + 14.62 \quad (9)$$

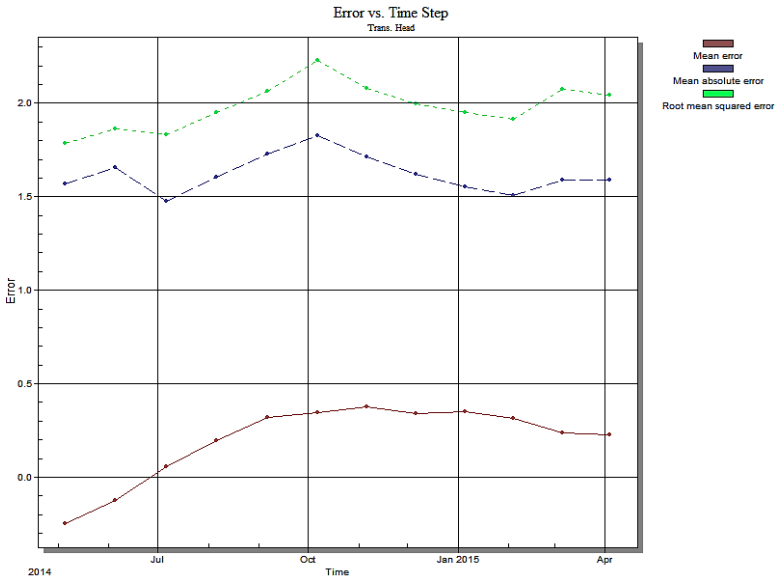

Figure 11. Error of month-to-month transient calibration process

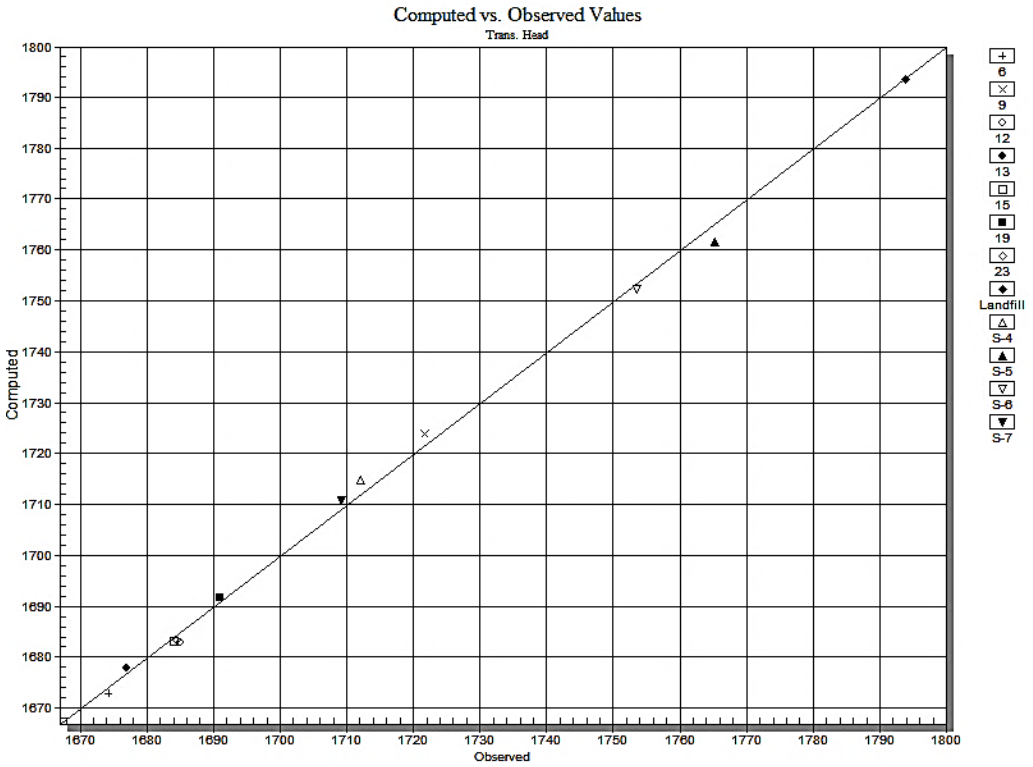

Figure12. Correlation between observed and calculated values in piezometer

MT3DMS qualitative model

Longitudinal distribution capability was determined about 30 m based on existing formulas and activation of MT3DMS transfer model, as well as the introduction of the initial and constant concentrations of 20000 PPM (15). In dispersion, the ratio of the horizontal to vertical dispersion (TRPT) and the ratio of the vertical to longitudinal dispersion (TRVT) within the aquifer were considered 1 and 0.1, respectively based on the information given in similar studies due to the lack of adequate data in the study area. The diffusion coefficient of main groundwater ions was then determined to be 1.5×10^{-9} m^2/s (27), which was used as diffusion coefficient in contaminant transport model (13). The method of Characteristics (MOC) is very effective in the elimination of numerical dispersion in severe convection problems. Third order TVD method, which is implemented by the overall current determinative, minimizes both numerical dispersion and artificial volatility. When the numerical dispersion not poses a major problem, and in cases where a network model is suitable or physical distribution is great, standard finite element method can be used more frequently (31). Accordingly, in the current study, the advection package of Standard Finite Difference Method was exerted. In a depleted environment, among the three types of absorption isotherms of Linear, Freundlich, and Langmuir, the first one was selected (30). Furthermore, chemical reactions were utilized in order to affect the chemical reactions in the study area. Considering the biodegradation factors, isothermal linear equilibrium (First-Order Irreversible Rate Reaction) method was also used in the present model (Table 4) (29, 13).

Table 4. Estimation of horizontal anisotropy, specific discharge, diffusion coefficient and porosity of each Solid octamerous material (7,19, 24)

Soil	Horiz Anis	Specific Yield	Long Disp	Porosity
Sand - Qt2	1	0.28333333	30	0.42
Schist	1	0.26	30	0.38
Marl	1	0.37	30	0.3825
Marl_Schist	1	0.315	30	0.3813
Conglomerate	1	0.05	30	0.25
K	1	0.12666667	30	0.2283
Ks	1	0.08175	30	0.2875
Qal	1	0.31	30	0.3875
OMn	1	0.37	30	0.3825

Based on the key results, pollution transfer modeling using MT3DMS code was found to be highly dependent on the calibration of the code MODFLOW model without the statistical bias of effective parameters on flow rate indicating that large-scale simulation is only run in the case of applying the primary three-dimensional and converged conceptual model. Changes in the numerical values of pilot horizontal hydraulic conductivity in the sensitivity analysis graphs claim about the effect of the boundaries with the dynamic flow in the West region of the study area (the aquifer) on the reduction of the overall level of groundwater modeling error (Figure 13). In cases with an insufficient number of exploratory cores, the conceptual geological model preparation based on the Solid justification method will then be effective if there is sufficient number of Grid horizontal layers.

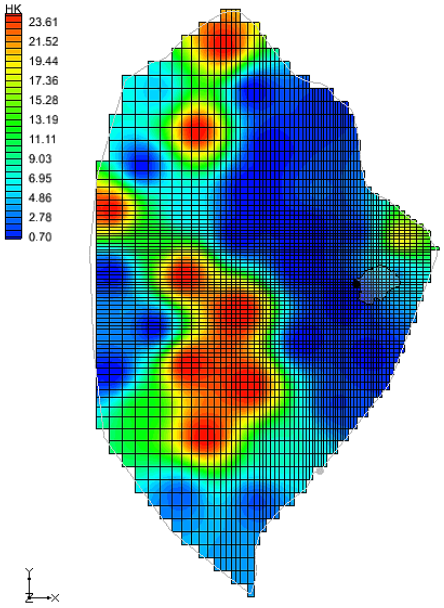

Figure 13. Increase in pilot hydraulic conductivity values in west of study area in the calibration step

Deep boreholes pollution adjacent to the waste disposal site within the city of Hamadan was not reported for benchmark indices, such as TDS or the indices without geological origin. The probability of existed pollution could therefore be attributed to the landfill area, which is located in the seasonal aquifers, and surface water flooding and its transformation through the feeding centers like springs across the plain. Based on the sampling experiments conducted in the boreholes around the Hamadan waste disposal sites, TDS index was reported in a standard level of Environmental Organization for deep boreholes; however, contamination was reported for the shallow boreholes (The upper unconfined aquifer) (21). In addition to TDS index, chloride index was applied as a benchmark, due to the lack of geological origin indicating that over-standard pollution was only observed in manually excavated and shallow boreholes near the waste disposal site. Hence, over-standard pollution was not observed in deep boreholes, as it was not reported in the previous papers. Although the assessment of groundwater pollution into the heavy elements revealed that all samples were contaminated with some elements, this contamination of samples can be attributed to the different origins from waste disposal sites, such as surface water flooding into groundwater through recharging areas.

The results of the present study indicated that the study area composed of a shallow quaternary aquifer in alluvial sediments, which was distinguished from deep aquifer by a low permeable conglomerate unit. In fact, the deep aquifer was constructed in the limestone bedrock whose thickness gradually increased toward the west. So, the leachate movement and expansion were inhibited into the main semi-confined aquifer. Only in cases where the surface flow flooding and severe rainfall occur, leachate migrates to the aquifer recharging streams. In quantitative aquifer modeling, the fixed and distinct amounts of Flow Budget ID were allocated to each five horizontal layers. Hence, the hydraulic exchange of each layer was determined based on its lower and upper layers (Table 5).

Table 5. MT3DMS chemical reactions Coefficients

Layer	1st Sorption Const	Rate Const (dissolved)	Rate Const (Sorbed)	Bulk Density
	M^3/mg	1/D	1/D	
1	0.00000585	0.0001	0.0001	53500
2	0.00000585	0.00005	0.00005	51500
3	0.00000585	0.000025	0.000025	49500
4	0.00000585	0.0000125	0.0000125	47500
5	0.00000585	6.25E-06	6.25E-06	45500

According to the overlay transfer of Solid characteristics to Grid, layers arrangement was consecutive thus enabling hydraulic exchange only by lower and upper layers. The results of the Flow Budget engine execution showed that despite the hydraulic exchange between different layers, this transaction does not take place due to the relatively impermeable formations in the area surrounding waste disposal sites, so the Grid cells will be in the nature of Dry. Therefore, the major contaminant transport toward the main aquifer was considered zero in the modeling process (Figure 14).

	IN		OUT	
CONSTANT CONCENTRATION:	0.000000		0.000000	
CONSTANT HEAD:	0.000000		0.000000	
WELLS:	0.000000		0.000000	
RIVERS:	0.000000		0.000000	
HEAD-DEPENDENT BOUNDARY:	0.000000		0.000000	
RECHARGE:	0.000000		0.000000	
MASS STORAGE (SOLUTE):	0.000000		0.000000	
[TOTAL]:	0.000000	mg	0.000000	mg

NET (IN - OUT): 0.000000
DISCREPANCY (PERCENT): 0.000000

Figure 14. Failure of the direct pollution transfer into the deep aquifer

A statistical summary of all areas defined in the Flow Budget indicated that the majority of volume within the study area was recharged from dynamic boundaries regarding structural issues rather than direct feed from the surface (Figure 15), which could be considered as the main cause of results in the current research (4).

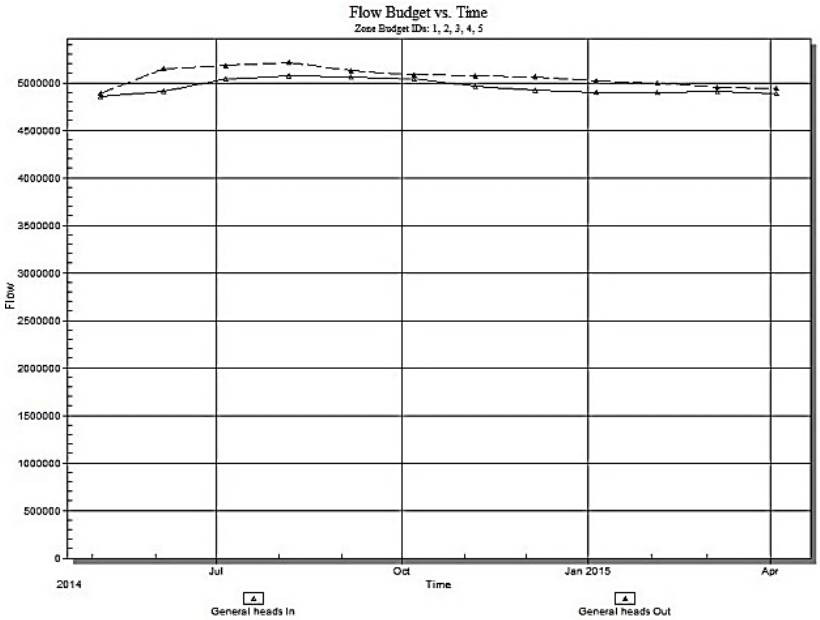

Figure 15. The volume fed from dynamic boundaries

It was also observed that in the municipal waste disposal sites of Hamadan, an impermeable conglomerate layer practically prevented the spread of pollution to the deep aquifer near the waste disposal site (Figures 16 and 17).

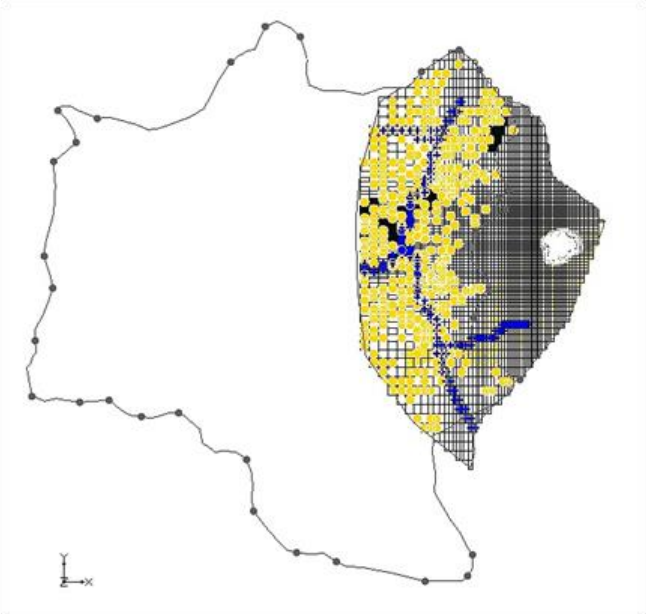

Figure 16. View of wells, waterway, and solid waste disposal sites versus active cells of calibration model in the first horizontal layer

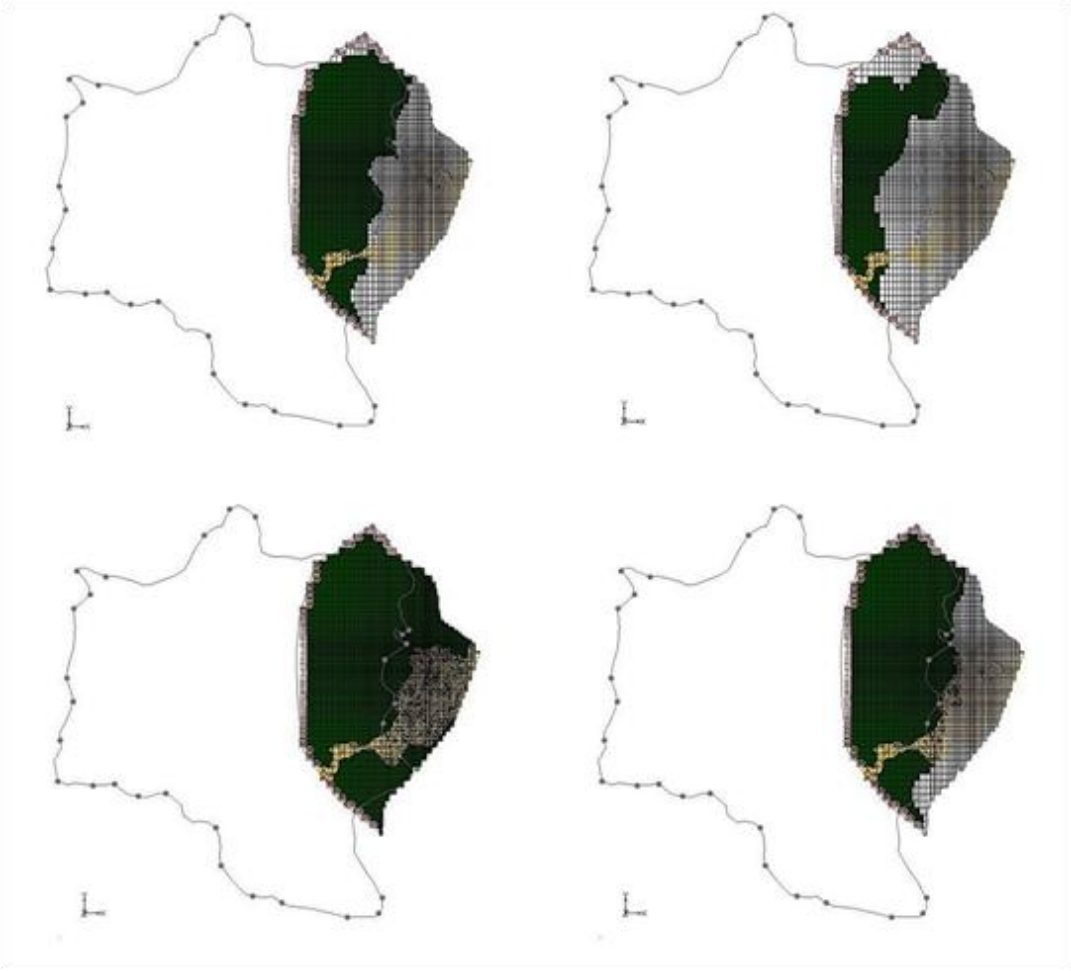

Figure 17. Water level demonstration in the four lower layers (permeable layer prevents direct contact between leachate and deep aquifer)

4. Conclusion

Based on the results of the study, geological structure of the landfill area had the greatest influence on the development of leachate pollution of municipal solid waste in traditional disposal sites. The spread of pollution to the deep aquifer near the waste disposal site was also found to be practically inhibited by an impermeable conglomerate layer in the municipal waste disposal. Deep boreholes pollution adjacent to the waste disposal site within the city of Hamadan was not reported for benchmark indices, and the probability of existing pollution was attributed to the landfill area, which is located in the seasonal aquifers, and surface water flooding. Also, the proximity of the landfill to the villages specified the necessity of further studies on the contamination of surface and subsurface resources. The results of the current study postulated that the study area was hydrogeologically composed of a shallow quaternary aquifer of alluvial formations, which is separated from deep aquifer by a low permeable conglomerate unit. The deep aquifer was also found to be composed of limestone formation which is highly cavernous and possessing porous media. It was further found that the leachate movement and expansion was inhibited into the main semi-confined aquifer. Thus, the migration of pollutant to deep aquifers can only occur in the area where the surface flow flooding and severe rainfall takes place.

Acknowledgments

The authors would like to thank Bu-Ali Sina University for providing support for the present project (the approval code: 2341997)

Conflict of interest

The Authors have no conflict of interest

References

1. Akhavan S, Abedi-Koupai J, Mousavi SF, Afyuni M, Eslamian SS. Abbaspour KC. Application of SWAT model to investigate nitrate leaching in Hamadan–Bahar Watershed, Iran. Agriculture, Ecosystems & Environment. 2010; 139(4): 675-688.
2. Akhavan S, Mousavi SF, Abedi-Koupai J, Abbaspour KC. Conditioning DRASTIC model to simulate nitrate pollution case study: Hamadan–Bahar plain. Environmental Earth Sciences. 2011; 63(6): 1155-1167.
3. Almasri MN, Kaluarachchi JJ. Modeling nitrate contamination of groundwater in agricultural watersheds. Journal of Hydrology. 2007; 343(3): 211-229.
4. Aquaveo Team. GMS: Solids to MODFLOW Command. Xmswiki. Accessed 22 October 2016. available from: https://www.xmswiki.com/wiki/GMS:Solids_to_MODFLOW_Command.
5. Aquaveo Team. GMS: Zone Budget. Xmswiki. Accessed 6 January 2016. available from: https://www. xmswiki. Com/wiki/GMS:Zone_Budget.
6. Batu V. Applied flow and solute transport modeling in aquifers: fundamental principles and analytical and numerical methods. Boca Raton, Florida, CRC Press, Taylor& Francis Group. 2005.
7. Bear J. Hydraulics of groundwater, McGraw-Hill series in water resources and environmental engineering. McGraw-Hill, New York. 1979.
8. Camba A, González-García S, Bala A, Fullana-i-Palmer P, Moreira MT, Feijoo G. Modeling the leachate flow and aggregated emissions from municipal waste landfills under life cycle thinking in the Oceanic region of the Iberian Peninsula. Journal of Cleaner Production. 2014; 67: 98-106.
9. Chain ESK, Walle FBD, Reston SN. Sanitary landfill leachates and their treatment. Journal of Environmental Engineering. 1976; 10:411-431.

10. Curry N, Pillay P. Biogas prediction and design of a food waste to energy system for the urban environment. Renewable Energy. 2011; 41: 200-209.
11. Dimitrijevic MD, Dimitrijevic MN, Vulovic D. 1:100,000 Geological Map of Iran. Ministry of Mines and Metals, Geological Survey of Iran, Tehran, Iran. 1971.
12. Domenico PA, Schwartz FW. Physical and Chemical Hydrogeology. 2nd edn, New York, John Wiley & Sons Inc. 1998.
13. Ehteshami M, Biglarijoo N. Determination of nitrate concentration in groundwater in agricultural area in Babol County, Iran. Journal of Research in Health Sciences. 2014; 2(4): 1-9.
14. Emami MH. 1:100,000 Geological Map of Iran, Sheet 5566. Ministry of Mines and Metals, Geological Survey of Iran, Tehran, Iran. 1994.
15. Fetter CW, Applied Hydrogeology Applied hydrogeology Visual Mod flow, Flownet and Aqtesolv student version software on CD-ROM ((Fourth edition edn.). Upper Saddle River: Prentice-Hall. 2001.
16. Gorsevski PV, Donevska KR, Mitrovski CD, Frizado JP. Integrating multi-criteria evaluation techniques with geographic information systems for landfill site selection: A case study using ordered weighted average. Journal of Waste Management. 2012; 32(2): 287-296.
17. Guerrero LA, Maas G, Hogland W. Solid waste management challenges for cities in developing countries. Journal of Waste Management. 2013; 33(1): 220-232.
18. H. R. W. A (Hamadan Regional Water Authority). Accessed 22 October 2016. available from: http://www.hmrw.ir/
19. Heath RC, Basic ground-water hydrology. Geological Survey Water-Supply Paper, 2220, Virginia, U.S. USGS Reston, V. A. 1983; pp. 86.
20. Hou D, He J, Lü C, Ren L, Fan Q, Wang J, Xie Z. Distribution characteristics and potential ecological risk assessment of heavy metals (Cu, Pb, Zn, Cd) in water and sediments from Lake Dalinouer, China. Ecotoxicology and Environmental Safety. 2013; 93: 135-144.
21. Khanlari GR, Taleb-Beydokhti A, Momeni AA, Ahmadi HR. Influence of Hamedan landfill leachate on groundwater. Journal of the Engineering Geological Society of Iran. 2013; 5(3-4): 81-92.
22. Kiddee P, Naidu R, Wong M H, Hearn L, Muller JF. Field investigation of the quality of fresh and aged leachate from selected landfills receiving e-waste in an arid climate. Journal of Waste Management, 2014; 34(11): 2292-2304.
23. Krook J, Svensson N, Eklund M. Landfill mining: A critical review of two decades of research. Journal of Waste Management. 2012; 32(3): 513-520.
24. Morris DA, Johnson AI. Summary of hydrologic and physical properties of rock and soil materials, as analyzed by the hydrologic laboratory of the U.S. Geological Survey, 1948-60, Virginia, U.S. Govt. Print. Off., Water Supply Paper. 1967; pp. 42.
25. Nakhaei M, Dadgar MA, Amiri V. Geochemical processes analysis and evaluation of groundwater quality in Hamadan Province, Western Iran. Arabian Journal of Geosciences. 2016; 9(5): 1-13.
26. Rosenshein JS, Moore JE. A history of hydrogeology in the United States Geological Survey. History of Hydrogeology. 2012; pp. 381.
27. Todd DK, Larry WM. Groundwater Hydrology, 3rd edn, New york, John Wiley & sons, NJ. 2005; pp. 636.
28. Trauth N, Schmidt C, Vieweg M, Oswald SE, Fleckenstein JH. Hydraulic controls of in- stream gravel bar hyporheic exchange and reactions. Water Resources Research. 2015; 51(4): 2243-2263.
29. Wick K, Heumesser C, Schmid E. Groundwater nitrate contamination: factors and indicators. Journal of

Environmental Management. 2012; 111(3): 178-186.

30. Zheng C, Wang PP. MT3DMS: a modular three-dimensional multispecies transport model for simulation of advection, dispersion and chemical reactions of contaminants in groundwater systems. Documentation and user's guide, Departments of Geology and Mathematics, University of Alabama. 1999; pp. 202.
31. Zheng C, Wang PP. MT3DMS: a modular three-dimensional multispecies transport model for simulation of advection, dispersion and chemical reactions of contaminants in groundwater systems. Tuscaloosa, Alabama. 1999; 35487-0338, U.S. Army Corps of Engineers, pp. 8-28.